"THE INTERPRETATION OF TIROS RADIATION DATA FOR PRACTICAL USE IN SYNOPTIC WEATHER ANALYSIS"

Lewis J. Allison
Goddard Space Flight Center

Guenter Warnecke*
Goddard Space Flight Center

*On leave from the Institut für Meteorologie und Geophysik der Freien Universität Berlin; Berlin, Germany, as National Academy of Sciences-National Research Council Research Associate

CONTENTS

Page

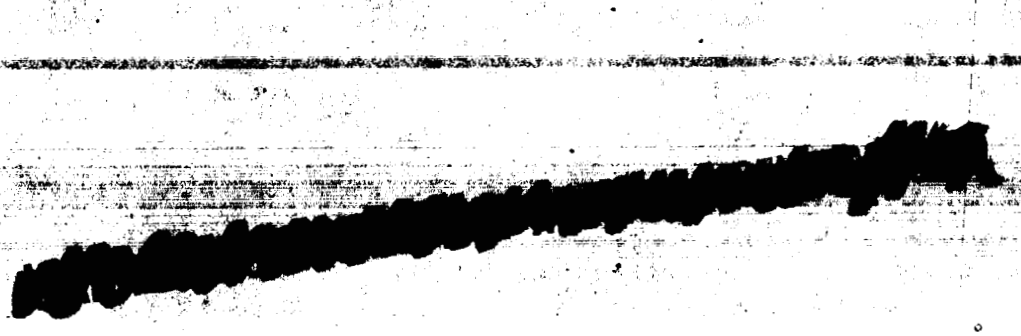

ABSTRACT

15246

Radiation data in the 8-12 micron atmospheric window and 6-6.5 micron water vapor absorption region acquired from the TIROS III meteorological satellite on 16 July 1961 are used to demonstrate some of the practical applications of satellite radiation data in synoptic weather analysis, looking to the near-future when similar data will become available for operational use. These applications include the mapping of horizontal cloud patterns at three different scales from meso- to quasi-global, the derivation of mean relative humidities in the troposphere over the United States, and the inference of vertical cloud structure along a cross section extending from Jamaica to British Columbia.

Each of the applications is discussed in the light of the corresponding conventional surface, upper air, vertical motion, relative humidity, precipitation, and cloud cover charts. Also, satellite television pictures are used in the discussion of meso- and macro-scale cloud mapping.

In general, a good synoptic correspondence is found between the conventional data and television pictures and the radiation data. Plausible mechanisms to explain several apparent discrepancies between the satellite and the conventional data are presented.

Author

LIST OF FIGURES

LIST OF FIGURES (Continued)

1. INTRODUCTION

Since the initial launch of the TIROS I meteorological satellite in April 1960, four satellites of the TIROS series have been used for radiation experiments by the National Aeronautics and Space Administration, namely, TIROS II, III, IV, and VII. In addition to the standard camera systems, these satellites carried a five-channel medium resolution radiometer, which measured the outgoing radiation of the atmosphere-earth system in five different spectral regions. A comprehensive series of publications has already described the details of the radiometer design, the data evaluation processes, and various results in many fields of atmospheric physics.[1,2,3,4,5,6] The purpose of this paper is to demonstrate some of the practical uses of satellite-detected radiation data in synoptic weather analysis.

2. THE TIROS RADIATION EXPERIMENT

The TIROS scanning radiometer consists of five channels, each channel being sensitive to a certain spectral region of the visible and infrared radiation which is reflected or emitted by the earth's surface and the atmosphere into space. The spectral sensitivities of the channels are as follows:

Channel	Spectral Region	Purpose
1	6.0 - 6.5 micron,	the ν_2 fundamental water vapor band
2	8 - 12 micron,	the atmospheric "window"
3	0.2 - 6 micron,	the total reflected solar radiation
4	7 - 30 micron,	the total outgoing infrared radiation
5	0.55-0.75 micron,	the response of the television camera systems

Contrary to the design of the television picture system of the TIROS satellites, the infrared radiation data are not restricted to the daylight portions of the orbits. Thus, with the current system of acquisition stations, radiation data are available for a maximum of 9 out of 14 orbits per day covering the quasi-globe. For example, the scan limits are approximately 55°N and S for TIROS III, and approximately 65°N and S for TIROS VII. Some examples of the large spectrum of applicability for this type of satellite information will be shown in the following

sections. It will become increasingly evident that the TIROS radiation data delineate significant meteorological characteristics of the atmospheric circulation, such as cloud regimes of cyclones and anticyclones, fronts, squall lines, tropical storms, monsoonal clouds, convergence zones and other important seasonal and diurnal synoptic features.

3. THE DERIVATION OF HORIZONTAL PATTERNS OF CLOUDINESS FROM THE TIROS RADIATION DATA

The radiation maps shown in this study were plotted and analyzed in terms of the basic quantity measured in the laboratory calibration, namely, the equivalent blackbody temperature, $T_{BB}(^{o}K)$. The values of T_{BB} should not be interpreted as the temperatures of viewed surfaces (although, for measurements in the 8-12 micron window, the difference between the two may be small under certain conditions). A T_{BB} measurement of a given radiometer channel is simply the temperature of a blackbody which, when filling the field of view, would cause the same radiation output as that which results from viewing the generally nonblackbody radiation from the earth and its atmosphere,[7,8]

There are some uncertainties involved in the interpretations of the T_{BB} values. For example, the earth's surface and cloud layers do not emit exactly as a blackbody and absorption and reemission by gases in the atmosphere can markedly change the characteristics of outgoing radiation from the underlying surfaces. The radiometer calibration as well as data conversion procedures can also inject some uncertainties into the analysis. Diagnostic methods have shown that the estimated relative accuracy for TIROS III, channels 1, 2 and 4 is $\pm 2^{o}K$, while the estimated absolute accuracy is $\pm 4^{o}$ to $\pm 8^{o}K$ up to orbits 118, 875 and 130, after applying corrections, respectively, after which the use of the data in terms of absolute measurements becomes questionable.[1] However, considering the complete lack of conventional synoptic data over considerable portions of the earth's atmosphere, the range of radiometer inaccuracy is not of major importance for global or meso-scale synoptic-radiation analyses.

In order to properly interpret the "window" radiation measurements, the field of view must also be carefully considered. The individual medium resolution radiometer sensor has an aperture of approximately 5 degrees (between the half-power points) which corresponds to a scan spot diameter of 40 miles, when it scans in the vertical and an elongated scan spot having an area approximately 10 times as large with a 58° scan nadir angle.[9] Hence, high scan nadir angle data recorded during each rotation of the satellite (9-12 rpm) will have a poorer resolution than low scan nadir angle data. When a homogeneous overcast cloud layer or clear skies over a sea or land region fills the field of view of the radiometer, a uniform interpretation of the T_{BB} values in terms of surface and cloud top temperatures, can be made. But if scattered to broken cloud decks of varying transparency are viewed, the radiation originating from the ground and the various cloud layers contribute to the integrated intensity detected by the satellite and make the interpretation of the measurement very difficult.[10] Other means such as conventional surface and upper air observations, in-flight reports, and satellite television pictures must be used to resolve the detailed horizontal and vertical cloud structure.

The two short-wave channels (3 and 5) can be used to detect the presence of highly reflective clouds provided that the earth's surface below provides sufficient contrast in reflectance. Areas covered by snow, ice or light-colored earth or desert sand can lead to misinterpretation of cloud fields. Use of the "solar" channels is restricted to the daylight portion of the earth in a manner similar to the television camera system, and the strength of reflected short-wave radiation becomes marginal at low solar elevation angles during sunset, sunrise, and the winter season at high latitudes.

Channel 2 which is not dependent on solar illumination and least effected by atmospheric absorption is best suited for the detection of cloud cover if corrections for instrumental degradation, small residual water vapor and ozone are applied.[1,6]

a. Meso-scale Clouds and Radiation Patterns

The capability of using the TIROS radiation data for a detailed cloud analysis is demonstrated in Figures 1 and 2. A cloud system at 10°N, 40°W on July 16, 1961 which was later identified as the early stage of Hurricane Anna, was selected for the analysis.[11]

Figure 1 shows the channel 2 radiation analysis for this storm. These data were acquired in the single open scanning mode and hence are located with greater accuracy than data acquired in either of the other two scanning modes, namely, the alternating open and closed scanning modes.[12] Each scan spot (cross mark) was hand plotted from a computer listing. The computer listing contains the geographical location of each scan spot, the scan nadir angle, the azimuth angles and simultaneous readings for all five radiation channels.[13]

The radiation analysis shown in Figure 1 was superimposed upon a TIROS television picture of the same storm (Figure 2). Good agreement was found between the television picture and the radiation field even out to the outer fringes of the photograph. An equivalent blackbody temperature difference of more than 50°K was indicated between the highest cloud tops (230°K) and the partly cloudy ocean area (282°K). By use of the Dakar, Senegal radiosonde sounding for 0000 GMT, 16 July 1961,[14] the 230°K T_{BB} value related to an "effective radiation height" of approximately 250 mb. (35,000 ft). The "effective radiation height" is defined as that height in the atmosphere where the ambient temperature equals the equivalent blackbody temperature (T_{BB}).

Several examples employing a detailed hand analysis of Hurricane Anna on 23 July 1961 are found in References 15 and 16.

b. Macro-Scale Clouds and Radiation Patterns

Besides the detailed structure of meso-scale cloud systems, the general distribution of cloudiness in the macro-scale is of vital interest to the synoptic meteorologist. The high correlation between the outgoing radiation within the water vapor window and cloudiness,[10,16,17,18] represents a most useful application of radiation data provided by the TIROS satellite. An example will be given in this section.

Figures 3 and 4 show the surface synoptic chart, and the corresponding 500 mb upper air chart analyzed by the National Meteorological Center, U. S. Weather Bureau, for 1200 GMT, July 16, 1961. The general weather pattern over the United States is characterized by an upper ridge and a weak surface high over the western states, a thermal surface low over the southwest, and an upper trough over the Mississippi Valley with well-developed thunderstorm and shower activity extending NE/SW from Maine to Texas. A second area of cyclonic activity is indicated by a frontal zone along the northwestern border states.

The observed surface cloud patterns for 1200 GMT are shown in the conventional nephanalysis chart (Figure 5). The broad region of cloudiness over the southeastern United States is confirmed by a mosaic of television pictures taken during orbit 61 (Figure 6). However, the synoptic explanation for the distinctive weather features over Louisiana, Mississippi, Alabama, Tennessee and Kentucky was singularly lacking in the surface analysis.

The channel 2 radiation analysis for orbits 57, 58 and 60 over the United States was drawn (Figure 7). This computer-produced map was printed on a 1:10 million scale, with a 40 degree scan nadir angle limitation. An average +4°K correction was applied to channel 2 T_{BB} values for instrumental degradation.[1]

The 230°K to 270°K isolines outline high-reaching clouds over the Appalachian Mountains and lower Mississippi Valley and a broad cloudy region along the northwest and north central United States border, southwestern Texas and the west coast of Florida.

The 280°K to 290°K isolines are associated with the clear to scattered clouds in the weak surface high and thermal surface low pressure regions over the central, southwest, and Gulf Coast states. Low-lying stratus and stratocumulus cloud decks over Indiana, Illinois, Michigan, Wisconsin and Minnesota and the scattered swelling cumulus and cumulonimbus clouds over central Texas occur within regions dominated by T_{BB} values of 270° to 280°K.

Based upon this TIROS radiation analysis (Figure 7), the mosaic of TIROS television pictures (Figure 6), and conventional cloud nephanalysis (Figure 5), a revised surface analysis was prepared (Figure 8).

A cold front, in the state of frontolysis was drawn in over Ohio, Kentucky, Tennessee and Arkansas. A pre-frontal squall line was shown, extending from Virginia through Tennessee, Alabama, Mississippi to Texas. An instability line, off the east coast was drawn crossing the north end of Florida (cumulonimbus activity) and merged with an easterly wave over western Cuba.

The cloudiness over northwest Florida, as shown in the television mosaic (Figure 6) is in good agreement with the channel 2 radiation data (Figure 7), with only a slight displacement; which was caused by a 3 to 6 hour data-recording time differential.

4. THE DERIVATION OF TROPOSPHERIC MEAN RELATIVE HUMIDITY FROM THE TIROS RADIATION DATA

Channel 1, of the medium resolution scanning radiometer is spectrally sensitive to emission within the fundamental water vapor band (6.0 to 6.5μ). F. Möller has developed a method of interpreting the radiation detected within this region in combination with channel 2, as a measure of the mean vertical relative humidity of the troposphere.[17,18,19]

This method which assumes a model atmosphere with a range of constant relative humidity in the vertical, provides an estimate of the mean relative humidity (±15%) for homogeneous overcast or clear sky condition[17] and tends to overestimate this parameter for nonhomogeneous scattered to broken cloud conditions.[20]

The following sections will describe an evaluation of the Möller technique over the United States on July 16, 1961 which complements an analysis performed over Europe on July 15, 1961.[17]

a. Method of Analysis

The TIROS III Evaluation Diagram for conversion of channel 1 and channel 2 to tropospheric mean relative humidity is presented in Figure 9. This diagram was constructed by W. R. Bandeen for a tropical model atmosphere and presented to the Workshop on the Uses of Satellite Data in Tropical Meteorology, Tallahassee, Florida in February 1963. Möller has shown that evaluation diagrams for various atmospheres are essentially equivalent[17] and it was deemed satisfactory for the purpose of this paper to utilize this diagram for middle latitudes as well. Since the determination of mean relative humidity becomes extremely inaccurate below 230°K, it was assumed that for values below 230°, the relative humidity was >90% (Figure 9). Corrections for degradation

and scan nadir angle were made in accordance with the TIROS III Radiation Data Users' Manual Supplement[1] and nomograms given by Möller and Raschke.[17]

The channel 1 and 2 grid print maps for orbits 57, 58 and 60 were computed-produced on a 1:10 million scale (composite) with a 40 degree scan nadir angle limitation. The 41° to 58° scan nadir angle data were used where data gaps existed in the 40° data. For a discussion of mapping scales and computer processing technique, see Ref. 12.

Figure 10 presents the final analysis of the satellite-derived mean relative humidity for July 16, 1961. Values of 70% and greater are shown in dark grey shading, 41% to 69% are enclosed in white, and 40% and less are shown in lighter grey shading.

b. Comparison with Conventional Moisture Patterns

Figures 11, 12, 13 show the moisture charts for the 300 mb, 400 mb and 500 mb level at 1200 GMT on July 16, 1961 as drawn from U. S. Weather Bureau radiosonde data.[14]

These conventional middle and upper tropospheric moisture charts and the satellite-derived moisture charts (Figure 10) show good agreement in outlining large regions of dryness (<20% R.H.) over the central and western two-thirds of the United States. Two dry tongues which were oriented N/S through central Texas, and NE/SW from the Gulf states to the Carolines are shown in both types of data. A third dry tongue over Western Texas, within the satellite-derived data does not occur in the conventional analysis but might be suggested within that area of sparse radiosonde data.

The moist region (70% and greater R.H.) in Figure 10 relate best to the integrated radiative contribution of the 300 mb, 400 mb and 500 mb moisture levels. The horizontal and vertical pattern of the moist high clouds over the cold front and the pre-frontal squall line, discussed previously, were confirmed with minor variations by the conventional and satellite-derived moisture analysis.

Figure 14 presents an analysis of the U. S. Weather Bureau (National Meteorological Center) mean relative humidity data for the 1000 mb to 500 mb layer for 1200 GMT. This chart shows the large dry and moist regions described above and in addition a well-defined moist tongue over Minnesota, Wisconsin, Michigan and the Great Lakes.

The satellite measurements would not be expected to be affected by the water vapor content in the layers below 500 mb as the atmosphere is largely opaque in the 6 to 6.5μ region in these layers.[7] Hence the low level moisture shown in Figure 14 does not contribute to the satellite derivation of mean relative humidity (Figure 10).

The preliminary moisture analysis presented above has indicated that the TIROS radiation data are capable of providing a gross picture of the upper tropospheric moisture patterns. Further work is required in view of the problem of instrumental degradation and the assumption of constant relative humidity in the vertical.[17]

c. Comparison with Vertical Motion Fields

Figure 15 shows the U. S. Weather Bureau Vertical Motion Chart at the 650 mb level for 1200 GMT, July 16, 1961. The following are some interrelationships between Figure 15 and Figures 7, 8, 10, 11, 12, 13, 14 and 16, which are of interest:

(1) The positive values (upward motion) of +0.1 to +0.9 cm/sec extending from central Texas to eastern Ohio, overlie the cloud layers of the cold front and squall lines (Figs. 7, 8), areas of high moisture content aloft (Figs. 10 thru 14), and major precipitation zones (Figure 16).

(2) The negative values (downward motion) of -0.6 to -1.7 cm/sec over Arizona and extending from New Mexico northeastward to Minnesota and of -0.1 to -1.0 cm/sec over California, Oregon, and Nevada generally coincide with clear to scattered clouds or

low-level cloud decks with dry air aloft. An area of subsidence overlies the 1000 to 500 mb moist tongue over Minnesota, Iowa, and Wisconsin, as previously described in Section 4(b).

When dry air overlies areas of upward motion such as over southern Idaho, eastern Nevada and Utah, east central Texas and Georgia, a weakening of the cumuloform-type cloud activity was noted.

A qualitative estimate of the large scale positive and negative vertical motion field could be made from Figure 10 if the generalized relationship between ascending motion, saturated air aloft, deep vertical cloudiness and precipitation on the one hand and descending motion, dry air aloft and suppressed vertical cloudiness on the other were used as a basis.[21,22,23]

5. THE DERIVATION OF VERTICAL CLOUD STRUCTURE FROM THE TIROS RADIATION DATA

As already indicated in Section 3(a), the TIROS channel 2 (8-12 micron) data, when converted into equivalent blackbody temperature (T_{BB}) may be interpreted to some extent as cloud top heights. By use of local radiosonde data, the derived T_{BB} value may easily be located in the vertical by means of the vertical temperature profile. In remote areas, however, climatological mean soundings may certainly be used as a first approximation.

The correlation between conventional cloud information and satellite radiation data can be demonstrated by the vertical cross-section in Figure 17. This cross-section extends from Kingston, Jamaica northwestward across the United States to Annette Island, Alaska on June 16, 1961 (see Figure 8), and is based upon conventional upper air data, at 1200 GMT.[14] The temperature field (^{o}C) including discontinuity lines from a squall line, frontal, and tropopause positions were presented. The humidity field was plotted and analyzed by means of temperature-dew point differences, as reported in the radiosonde data.[14] In a more schematic manner, the probable cloud distribution was drawn for temperature-dewpoint differences of $3^{o}C$ or less and from conventional surface and pilot weather reports.

The most apparent features within the cross section (Figure 17) are the pre-frontal squall line over northern Alabama, the cold front over northwestern Tennessee, the cold front over Montana, and their corresponding heavy cloud systems, reported by surface observations as well as being derivable from the radiosonde humidity information. Included in this cross-section is a heavy solid line with small open circles which indicates the effective

radiation height of channel 2, orbits 56, 57, 58, and 60 on July 16, 1961. The circles give the actual values of T_{BB} exactly along the base-line of the cross-section. The full dots represent the corresponding values over the radiosonde station location. A larger discrepancy between both values occurs only with regard to Little Rock, Arkansas, as the cross-section passes the cold front just in a portion of weakest intensity (see Figures 5, 8) of cloud development, while much higher reaching clouds are reported in the area surrouding the radiosonde station. The relative dryness indicated by the Little Rock radiosonde measurement may be interpreted as having occurred between several high reaching cloud cells rather than within the most intense frontal cloud system. Therefore the schematic indication of the frontal clouds was drawn up to the effective radiation height determined by the satellite measurement. It should be noted that while the cross-section is valid for 1200Z, the satellite data were recovered from approximately 0800 GMT, for orbit 56 over Cuba to 1500 GMT, for orbit 60 along the U. S. - Canadian border. Thus, for the central portion of the section, roughly between Tennessee and South Dakota, the conventional data and the satellite data are quasi-synoptic, and hence some deviations between conventional and satellite data are apparent. Therefore, in order to make the cross-section representative for the area rather than for a single spot of the frontal system, the cloud system of the cold front over Little Rock was drawn in to approximately 22,000 feet. The squall line and cold frontal cloud decks which were primarily based upon the humidity profiles over Nashville, Tennessee and Glasgow, Montana were found to be in good agreement with the TIROS effective radiation heights.

Northwest of Edmonton, in an area where various cloud layers of stratocumulus, altocumulus and cirrus were reported, the effective radiation heights appeared between the cirrus clouds at 350 mb and the cloud decks which extended from the surface to 500 mb. The characteristics of the channel 2 emission from scattered to broken cirrus clouds have been discussed previously by Fritz and Winston[10] and Rao and Winston.[24]

In the clear area around Rapid City, North Dakota, the indicated T_{BB} values of 7.5°C differ from the 20°C shelter temperature. In this case, the thin cloud or moist layer at 650 mbs is the primary cause of the temperature difference although ozone absorption and/or possibly particulate matter near the tropopause at about 13 km can also act to decrease the channel 2 T_{BB} temperature.[24]

6. QUASI-GLOBAL SCALE CLOUD DISTRIBUTION

The spectrum of applicability of the TIROS radiation data extends from the meso-scale to the quasi-global scale. Figure 18 is the world-wide synoptic-radiation analysis on July 16, 1961 in which synoptic information from world weather centrals were utilized.[25] Channel 2 T_{BB} values from 7 orbits (56, 57, 58, 60, 61, 62, 63) were composited and analyzed on a 1:20 million map scale using a 58° scan nadir angle limitation. Orbit 59, which was missing, accounts for the gaps over Africa and the central Pacific.

The synoptic analyses were adjusted to approximate orbital times starting at 0600 GMT and ending 2000 GMT, approximately. The portion of the map lying east of the diagonal running from 20°S, 45°E to 20°N, 90°E consists largely of nighttime data while the area west of this line consists of daylight recording.

At this time, the Northern Hemisphere is close to its annual heat maximum; the Southern Hemisphere being in mid-winter season with its usual strong cyclonic activity extending far northward toward the equator. The darkest grey shading showing the highest temperatures indicate clear to scattered cloud cover (few small cumulus or very transparent cirrus patches). We find these T_{BB} values of 290°K and greater, over the Sahara Desert, Saudi-Arabia, Asia Minor, Iran, Turkmen, Spain, and the deserts of Southwest Africa. The semi-permanent subtropical highs (T_{BB} values between 270°K and 280°K indicate large areas of clear to scattered clouds).

The lightest grey shading in this figure is associated with the lowest equivalent blackbody temperature (<240°K) and

consequently with the highest amount of high-reaching cloudiness. The areas of high reaching cloudiness represent the frontal zones of both hemispheres as well as the heavy monsoonal cloudiness over Southern Asia and four tropical disturbances. We can distinguish the frontal system over the southeastern United States (see Figures 5 and 8), the polar front over Western and Central Europe and a very extended frontal band reaching from Japan northeastward to the Gulf of Alaska. Minimum T_{BB} values as low as 225°K, indicate that these cloud systems extend upward toward the tropopause. Similar minimum values occur within the cloud mass of the tropical storm "Flossie" over the Philippines. The tropical storms "Kathleen" and "Liza" off the west coast of Mexico are in their decay stage and T_{BB} values of 230° and greater are indicated. Over the tropical Atlantic Ocean, a singular cloud mass near 10°N and 40°W was identified as the early stage of hurricane "Anna", which was presented in detail in Figure 1.

The cloudiness along the tropical convergence zone is represented by cold equivalent blackbody temperature (225°K to 260°K) over Central America, Northern Brazil, the Western African coast, north of Lake Victoria, east of the coast of Somaliland and between 10°N and the equator over theCentral Pacific.

The high-reaching clouds over the Indian subcontinent and the adjacent Bay of Bengal and Indian Ocean and Southeast Asia clearly show the dense cloud outlines of the southwest moonsoon in those regions.

Over the Southern Hemisphere, we can delineate cloud zones of the intensive storm tracks extending northward to Uruguay, close to the southern tip of Africa, and affecting southern Australia and particularly New Zealand.

7. CONCLUSION

The results of this study indicate that a wealth of synoptic weather information can be derived or measured directly from the conventional TIROS radiation data.

In the future, polar-orbiting, earth-oriented meteorological satellites with their global data coverage and simpler radiometer scanning geometry will provide an even greater capability for a world-wide real-time synoptic-radiation weather watch.

8. ACKNOWLEDGEMENTS

The authors would like to thank Dr. William Nordberg, Mr. William R. Bandeen and Mr. Virgil Kunde of the Goddard Space Flight Center for their comments and suggestions.

We are particularly indebted to Mr. Thomas I. Gray, Jr. of the Meteorological Satellite Laboratory, U. S. Weather Bureau and Captain Robert W. Fett, U. S. Air Force, for their contributions and assistance in the preparation of this article. It is of interest to note that the double frontal model depicted throughout the Southern Hemisphere in the revised surface-radiation analysis shown in Figure 18, was largely the work of Thomas I. Gray, Jr., (Reference 25).

9. REFERENCES

1. W. R. Bandeen, R. E. Samuelson and I. P. Strange, "TIROS III Radiation Data Users' Manual Supplement: Correstion models for Instrumental Response Degradation", NASA, Goddard Space Flight Center, Greenbelt, Md., December 1, 1963.

2. W. R. Bandeen, B. J. Conrath, W. Nordberg and H. P. Thompson, "A Radiation View of Hurricane Anna from the TIROS III Meteorological Satellite", Proc. First Intl. Symposium on Rocket and Satellite Meteorology, Wash., D.C., April 1962, Amsterdam: North-Holland Publishing Co., 1963.

3. "TIROS IV Radiation Data Catalog and Users' Manual," NASA/Goddard Space Flight Center, Greenbelt, Md., 15 December 1963.

4. D. Q. Wark and J. S. Winston, "Application of Satellite Radiation Measurements to Synoptic Analysis and to Studies of Planetary Heat Budget", Proc. First Intl. Symposium on Rocket and Satellite Meteorology, Washington, D. C., April 1962, Amsterdam: North-Holland Publishing Co., 1963.

5. W. Nordberg, W. R. Bandeen, V. Kunde and G. Warnecke, "Stratospheric Temperature Patterns Based on Radiometric Measurements from the TIROS VII Satellite", NASA TN (to be published), Goddard Space Flight Center, Greenbelt, Md.

9. REFERENCES (Continued)

6. D. Q. Wark, G. Yamamoto and J. H. Lienesch, "Methods of Estimating Infrared Flux and Surface Temperature from Meteorological Satellites", Journal of the Atmospheric Sciences, Vol. 19, (5), 369-384, Sept. 1962.

7. Hanel, R. A. and D. Q. Wark, "Physical Significance of the TIROS II Radiation Experiment", NASA Technical Note D-701, Dec. 1961.

8. "TIROS III Radiation Data Users' Manual", NASA/Goddard Space Flight Center, Greenbelt, Maryland, August 1962.

9. T. Fujita, "Outline of a Theory and Examples for Precise Analysis of Satellite Radiation Data", Mesometeorology Project Research Paper 15, University of Chicago, Feb. 1963.

10. S. Fritz and J. S. Winston, "Synoptic Use of Radiation Measurements from Satellite TIROS II", Monthly Weather Review, Vol. 90, 1, (1962).

11. S. Fritz, "Satellite Pictures and the Origin of Hurricane Anna", Monthly Weather Review, Vol. 90, pp. 507-513, Dec. 1962.

12. W. R. Bandeen, "TIROS II Radiation Data Users' Manual Supplement," NASA/Goddard Space Flight Center, Greenbelt, Maryland, May 15, 1962.

13. "TIROS III Radiation Data Catalog," NASA/Goddard Space Flight Center, Greenbelt, Maryland, 15 December 1962.

9. REFERENCES (Continued)

14. Daily Series, Synoptic Weather Maps, Part II, Northern Hemisphere Data Tabulations, Daily Bulletin, July 16, 1961, U. S. Department of Commerce, Weather Bureau, Government Printing Office, Washington, D. C.

15. T. Fujita and J. Arnold, "The Decaying Stage of Hurricane Anna of July 1961, as Portrayed by TIROS Cloud Photographs and Infrared Radiation from the Top of the Storm", Mesometeorology Project, Research Paper 28, University of Chicago, November 1963.

16. W. Nordberg, "Research with TIROS Radiation Measurements", Astronautics and Aerospace Engineering, Vol. 1, No. 3, pp. 76-83, April 1963.

17. F. Möller and E. Raschke, "Evaluation of TIROS III Radiation Data", Interim Report No. 1, Ludwig-Maximilians-Universität, Meteorologisches Institut, München, Germany, July 1963.

18. F. Möller, "Some Preliminary Evaluation of TIROS II Radiation Measurements", Universität München, Meteorologisches Institüt, January 15, 1962.

19. F. Möller, "Atmospheric Water Vapor Measurements at 6-7 Microns from a Satellite", Planet Space Science, Vol. 5, pp. 202-206, Pergamon Press, Great Britain, 1961.

20. W. R. Bandeen, Private Correspondence, June 1964.

9. REFERENCES (Continued)

21. L. A. Vuorela, "On the Air Flow Connected with the Invasion of Upper Tropical Air over Northwestern Europe", Geophysics, Vol. 4, pp. 105-130 (1953).

22. L. A. Vuorela, "A Study of Vertical Velocity Distribution in some Jet Stream Cases over Western Europe," Geophysics, Vol. 6(2), pp. 68-90, (1957).

23. E. Paul McClain, "The Case of March 9, 1962 - An Investigation of the Structure of Cloud and Weather Systems Associated with Cyclones in the United States", Scientific Report No. 11, University of Chicago, Sept. 1963.

24. P. K. Rao and J. S. Winston, "An Investigation of Some Synoptic Capabilities of Atmospheric"Window" Measurements for Satellite TIROS II", Journal of Applied Meteorology, Vol. 2, 1 (1963).

25. L. J. Allison, T. I. Gray, Jr., and G. Warnecke, "A Quasi-Global Presentation of TIROS III Radiation Data", NASA SP 53 - (November 1964), Goddard Space Flight Center, Greenbelt, Maryland

FIGURE CAPTIONS

1. Analysis of channel 2 radiation data of the early stage of Hurricane Anna, July 16, 1961 (open mode data only) hand plotted from listings.

2. Composite analysis of channel 2 radiation data (listings) and a gridded television picture of the early stage of Hurricane Anna.

3. The surface synoptic chart 1200 GMT, July 16, 1961 over the United States (National Meteorological Center, U. S. Weather Bureau).

4. 500 mb constant pressure chart over the United States, at 1200 GMT, July 16, 1961.

5. Conventional cloud analysis over the United States at 1200 GMT, July 16, 1961.

6. Mosaic and nephanalysis of TIROS III television pictures over the United States recorded during orbit 61, 1655 GMT, July 16, 1961.

7. Channel 2 radiation analysis (T_{BB}; ^{o}K) over the United States recorded during orbits 57, 58, and 60, July 16, 1961 from 1000 GMT to 1500 GMT.

8. Revised surface analysis over the United States at 1200 GMT, July 16, 1961 (Diagonal line indicates path of vertical cross section in Figure (17)).

9. TIROS III evaluation diagram for conversion of channel 1 and channel 2 T_{BB} data to tropospheric mean relative humidity (%). For a pair of simultaneous channel 2 and channel 1 values, the mean relative humidity is determined by their intersection. For example, for channel 2 ($260^{o}K$) and channel 1 ($235^{o}K$), the Mean Relative Humidity = 60%.

FIGURE CAPTIONS (Continued)

10. Analysis of satellite-derived mean relative humidity (%) for orbits 57, 58, and 60 on July 16, 1961.

11. Analysis of conventional 300 mb relative humidity (%) at 1200 GMT, July 16, 1961, over the United States.

12. Analysis of conventional 400 mb relative humidity (%) at 1200 GMT, July 16, 1961, over the United States.

13. Analysis of conventional 500 mb relative humidity (%) at 1200 GMT, July 16, 1961, over the United States.

14. Analysis of conventional 1000 mb to 500 mb mean relative humidity (%) at 1200 GMT, July 16, 1961, over the United States.

15. Analysis of vertical motion (650 mb level) in cm/sec at 1200 GMT, July 16, 1961.

16. Analysis of precipitation amounts (inches) at 1200 GMT ($\pm$1 hr), July 16, 1961, over the United States.

FIGURE CAPTIONS (Continued)

17. Vertical cross-section over the United States at 1200 GMT, July 16, 1961. Temperatures are in °C. Thermal discontinuities are indicated in a conventional manner. The humidity distribution is for practical reasons presented by isolines of temperature-dewpoint differences in °C. Grey shades differentiate the significant moist zones (light grey: more than 20° temperature-dewpoint difference; medium grey: less than 5° temperature-dewpoint difference; dark grey indicates schematically cloud systems inferred by conventional and by satellite data). The heavy solid line with dots superimposed represents the effective radiation heights derived from equivalent blackbody temperature measurements of channel 2 and conventional radiosonde data. The plotting model used shows air temperature to the left of the black dot and air temperature, dewpoint temperature difference on the right.

18. Composite map of channel 2 radiation data and revised surface synoptic analysis on a quasi-global scale for July 16, 1961.

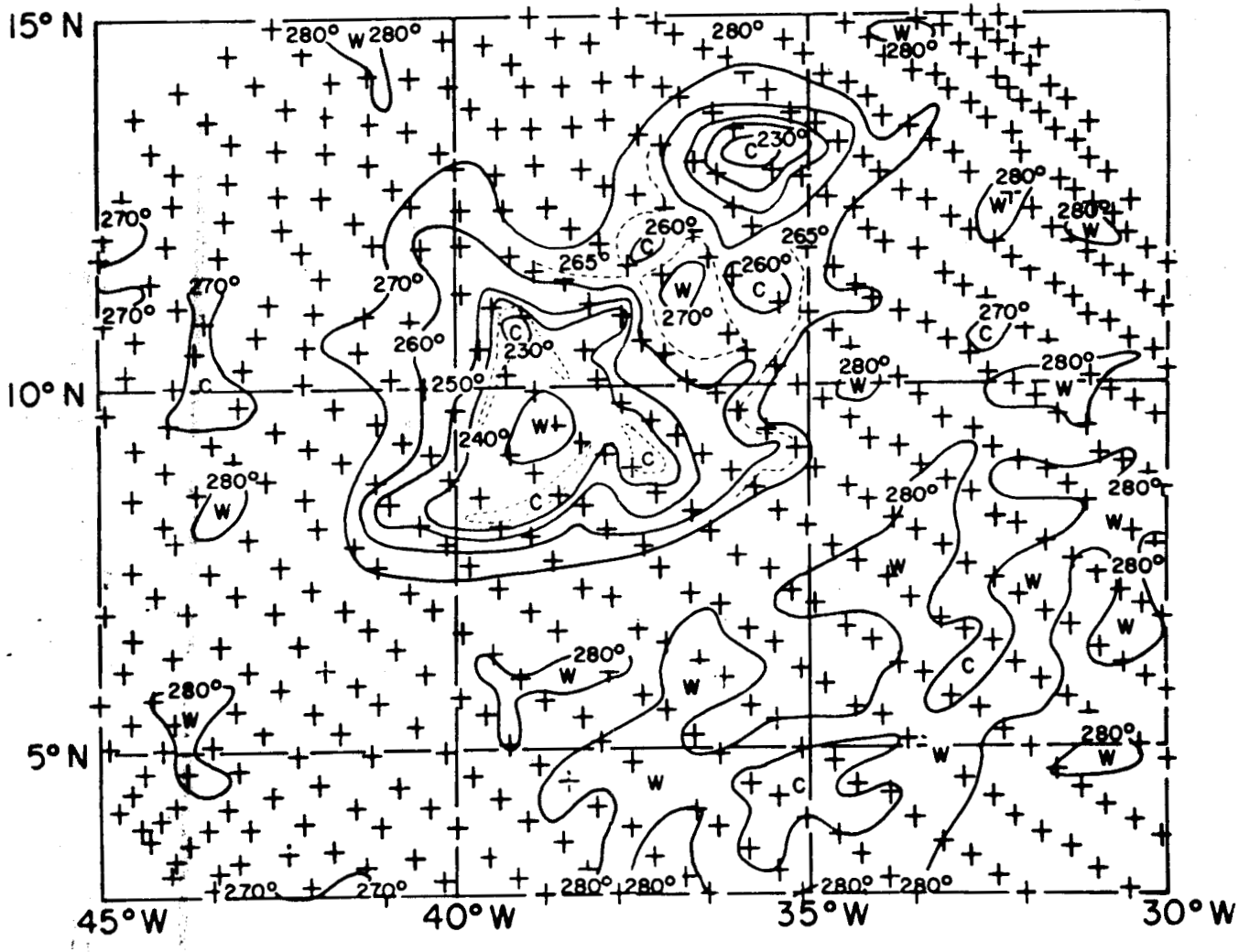

Fig. 1

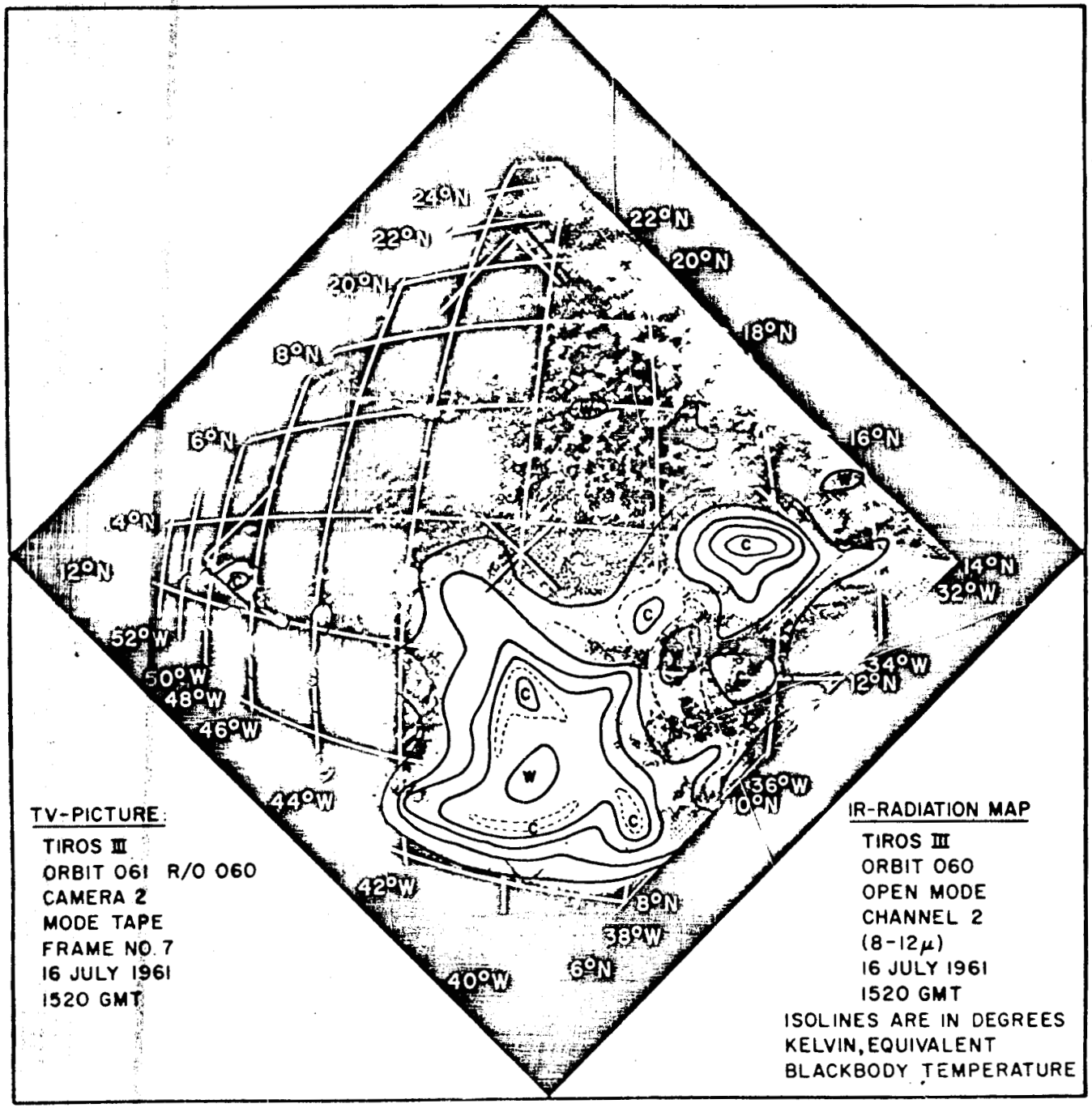
24°N
22°N
20°N
18°N
16°N
14°N
12°N
10°N
8°N
6°N
4°N
2°N
0°N
52°W
50°W
48°W
46°W
44°W
42°W
40°W
38°W
36°W
34°W
32°W
C
W
TV-PICTURE:
TIROS III
ORBIT 061 R/O 060
CAMERA 2
MODE TAPE
FRAME NO. 7
16 JULY 1961
1520 GMT
IR-RADIATION MAP
TIROS III
ORBIT 060
OPEN MODE
CHANNEL 2
(8-12μ)
16 JULY 1961
1520 GMT
ISOLINES ARE IN DEGREES
KELVIN, EQUIVALENT
BLACKBODY TEMPERATURE

Fig. 2

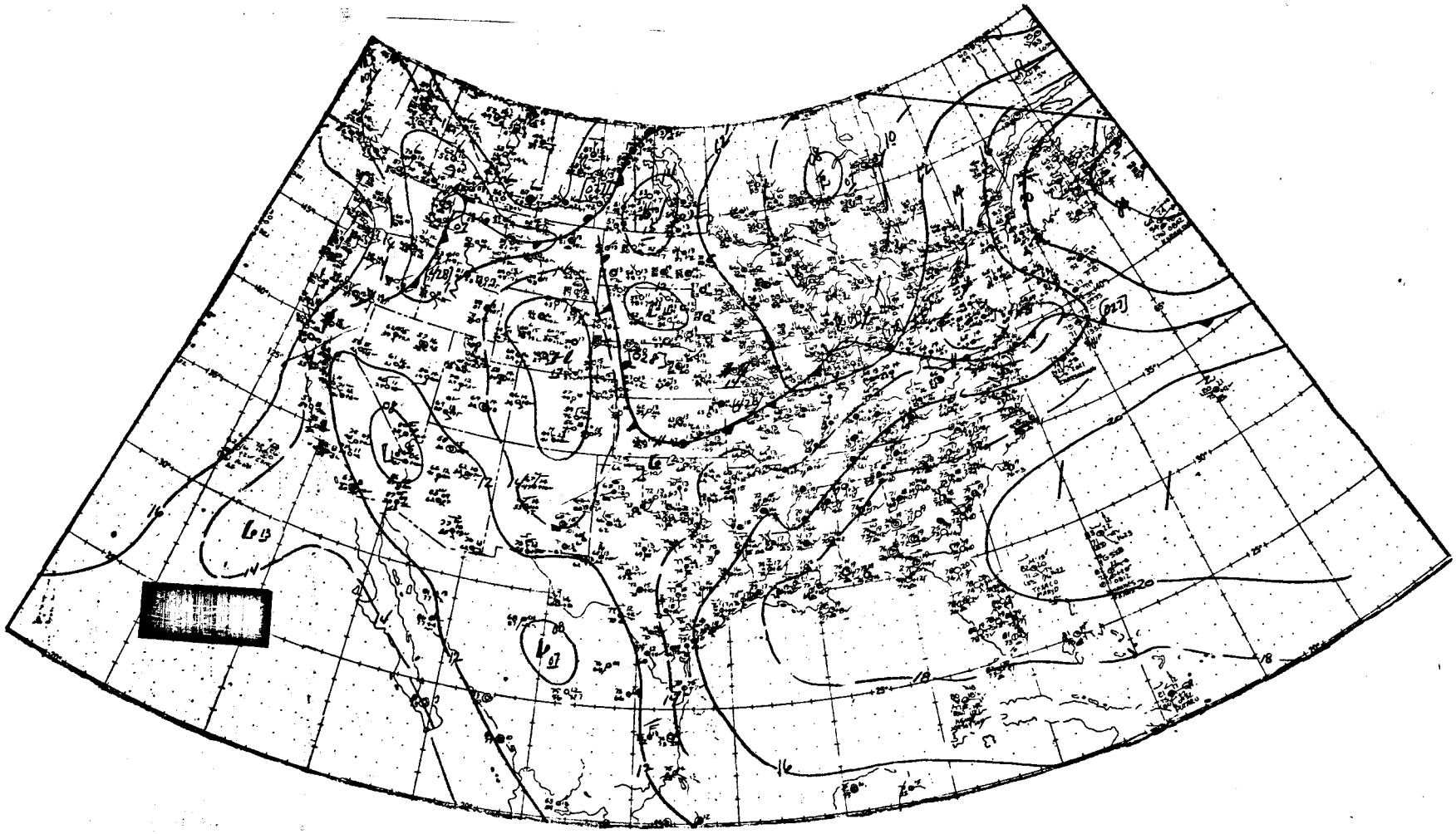

Fig 3

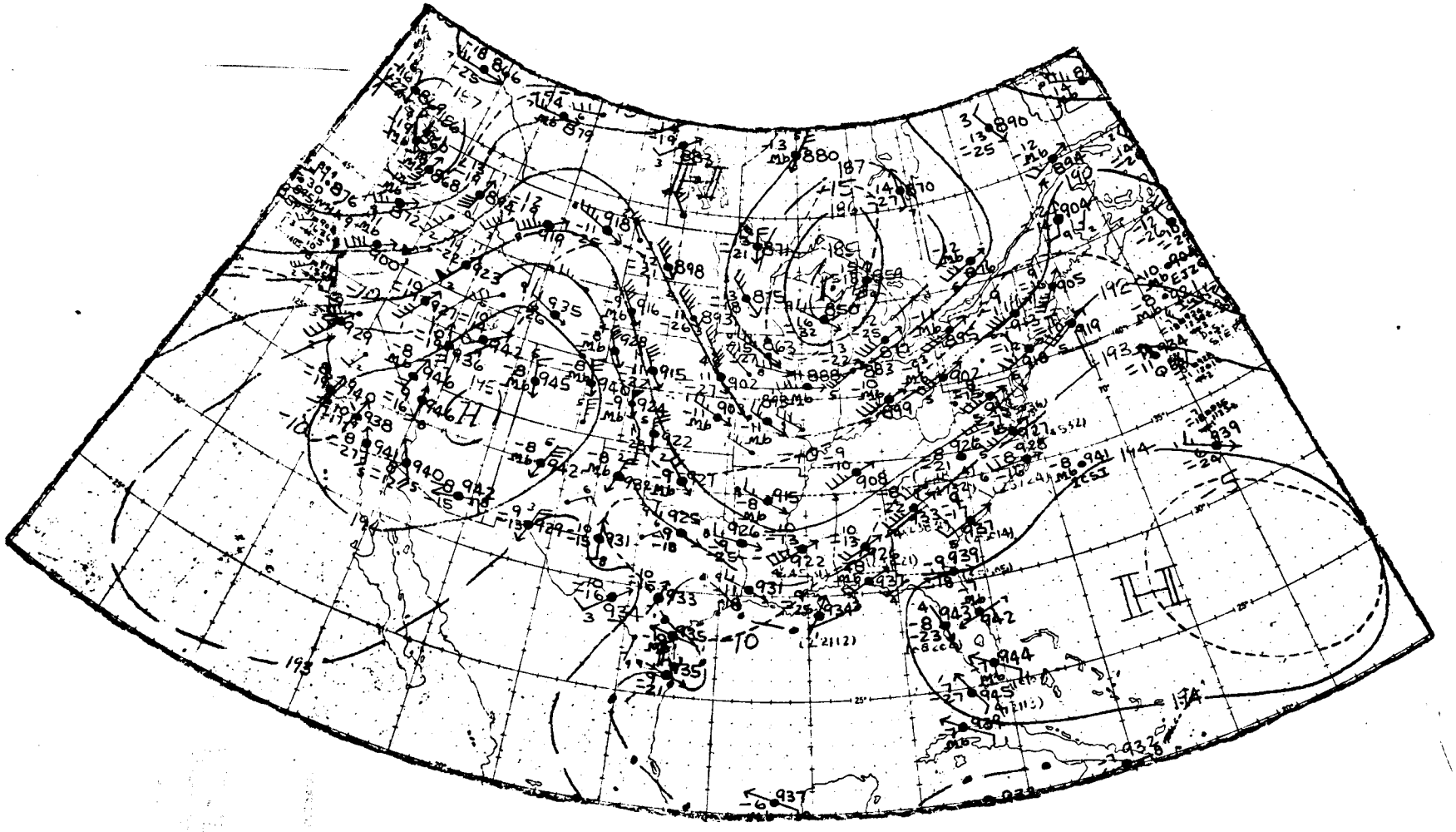

Fig. 4

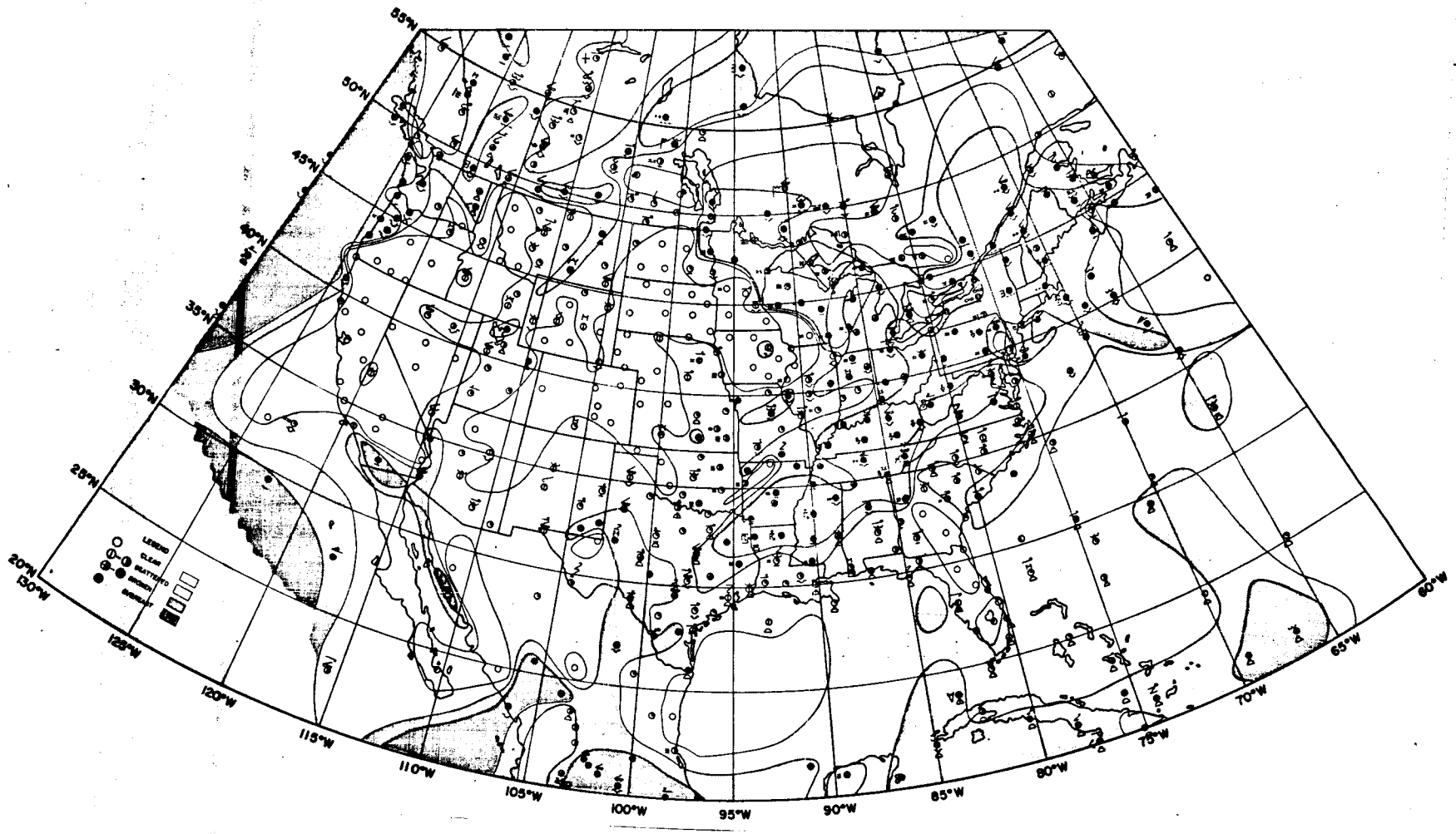
55°N
50°N
45°N
40°N
35°N
30°N
25°N
20°N
130°W
125°W
120°W
115°W
110°W
105°W
100°W
95°W
90°W
85°W
80°W
75°W
70°W
65°W
60°W
LEGEND
P.E.
PLUTONIC
VOLCANIC
SEDIMENT

Fig. 5

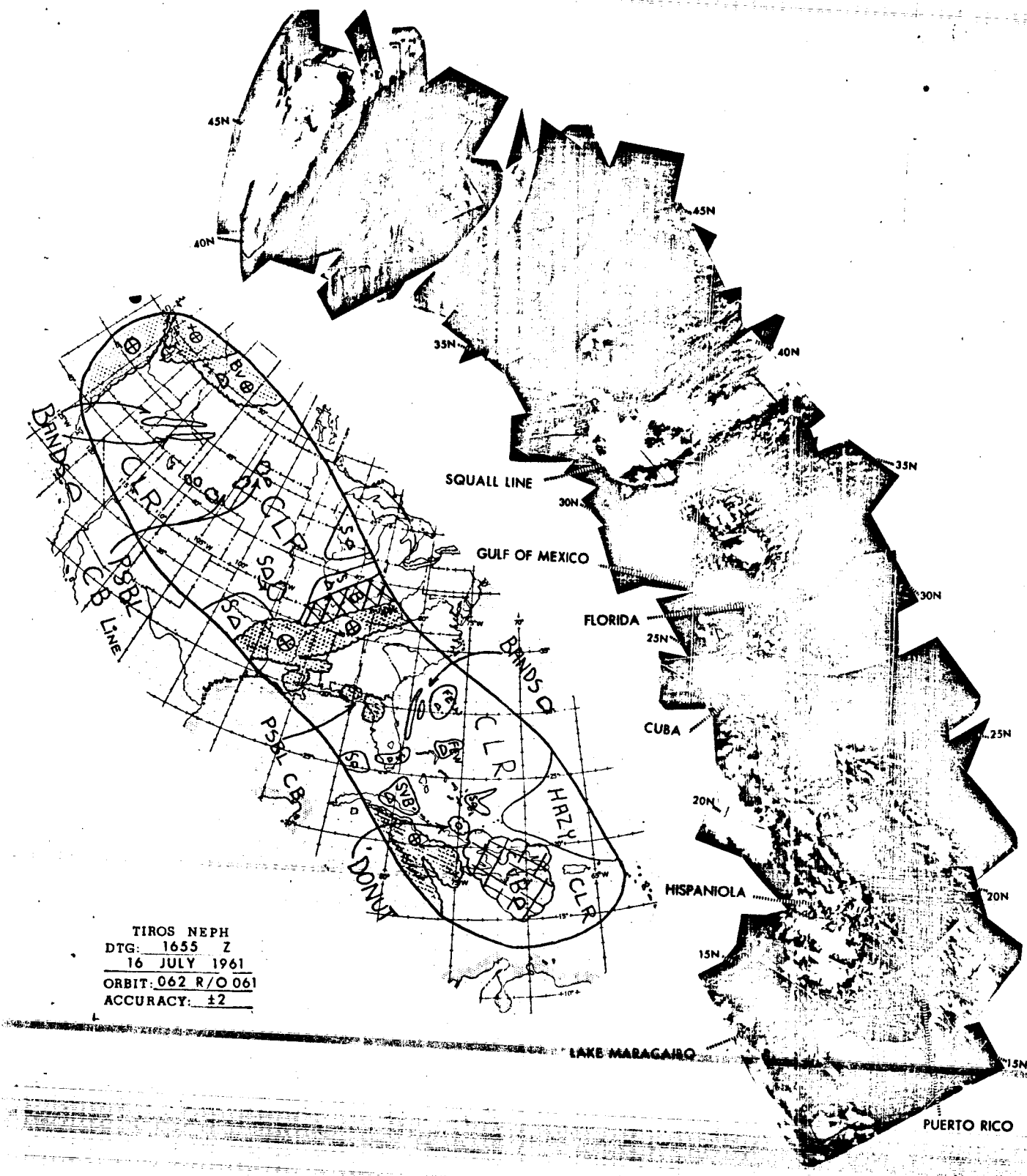
45N
40N
35N
30N
25N
20N
15N
SQUALL LINE
GULF OF MEXICO
FLORIDA
CUBA
HISPANIOLA
LAKE MARACAIBO
PUERTO RICO
BANDS
CLR
HAZY
DCLR
PSBL CB
CB LINE
DONW
TIROS NEPH
DTG: 1655 Z
16 JULY 1961
ORBIT: 062 R/O 061
ACCURACY: ±2

Fig. 6

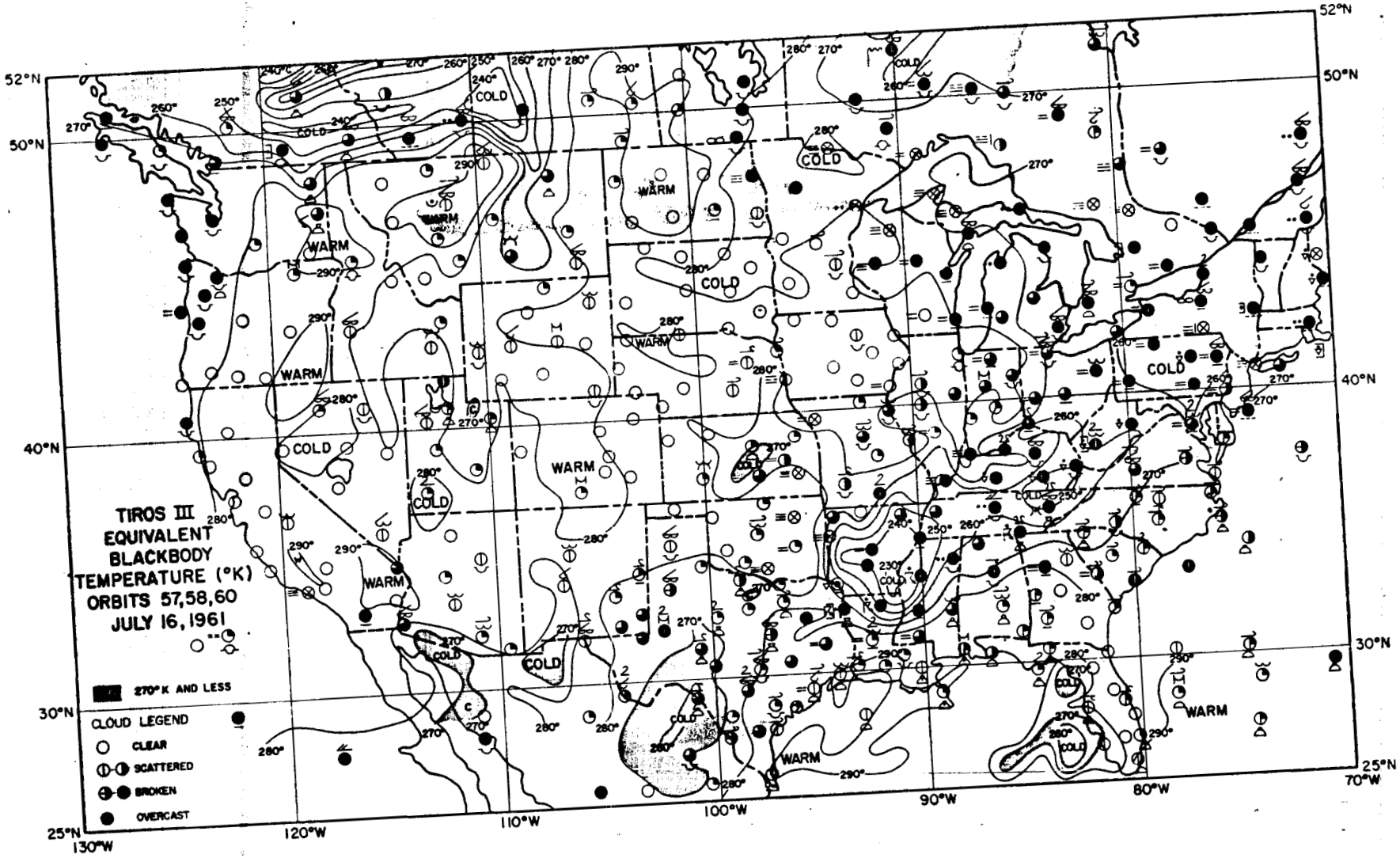
TIROS III
EQUIVALENT
BLACKBODY
TEMPERATURE (°K)
ORBITS 57,58,60
JULY 16, 1961
270°K AND LESS
CLOUD LEGEND
CLEAR
SCATTERED
BROKEN
OVERCAST
COLD
WARM
52°N
50°N
40°N
30°N
25°N
130°W
120°W
110°W
100°W
90°W
80°W
70°W

Fig. 7

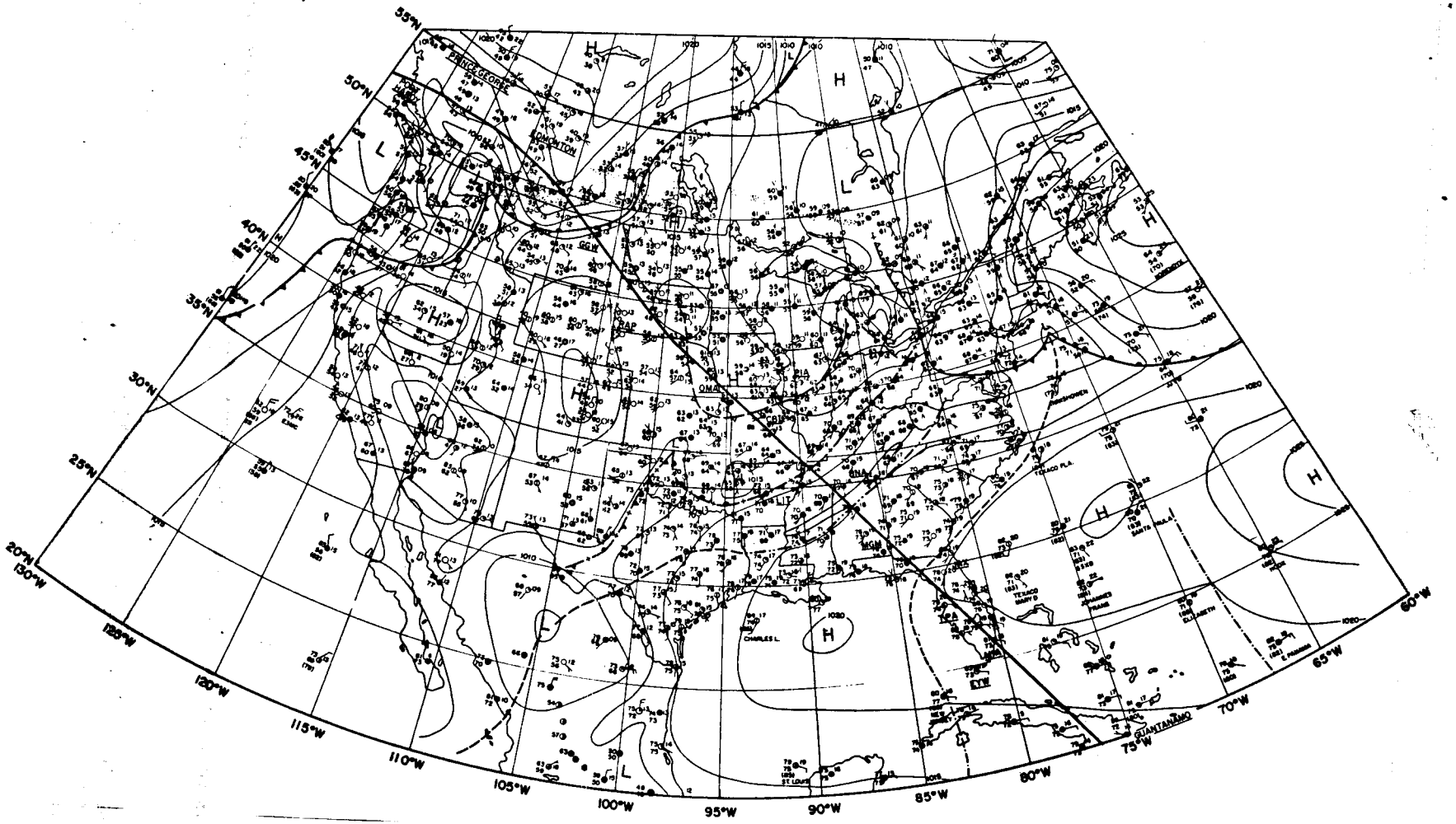
55°N
50°N
45°N
40°N
35°N
30°N
25°N
20°N
130°W
125°W
120°W
115°W
110°W
105°W
100°W
95°W
90°W
85°W
80°W
75°W
70°W
65°W
60°W
PRINCE GEORGE
EDMONTON
OMAHA
ST LOUIS
CHARLES L.
TEXARKANA
GUANTANAMO

Fig. 8

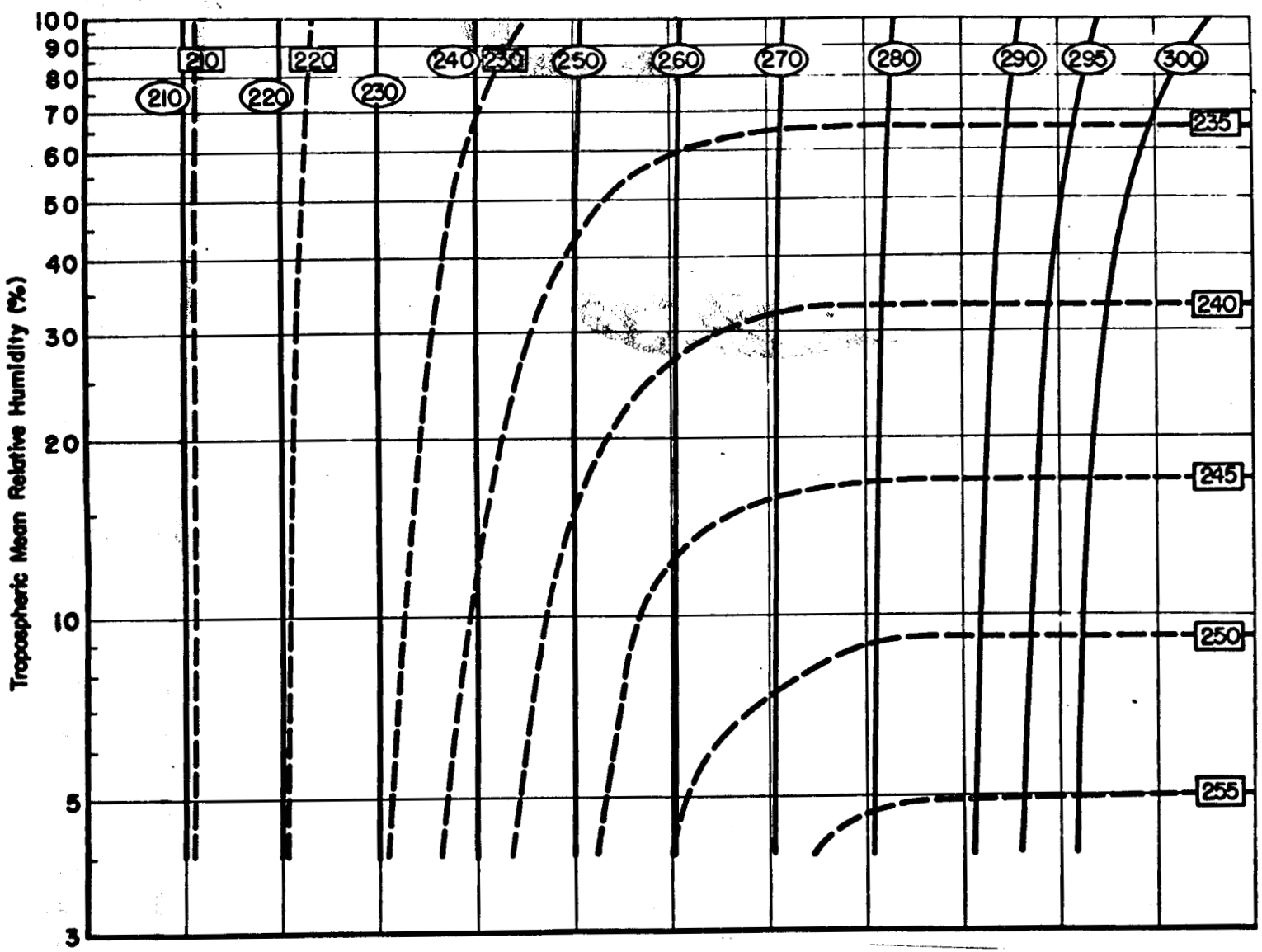

TIROS III EVALUATION DIAGRAM

EQUIVALENT BLACKBODY TEMPERATURES (°K)

CHANNEL 1 (6 - 6.5μ) — — —

CHANNEL 2 (8-12μ) ——————

Fig 9

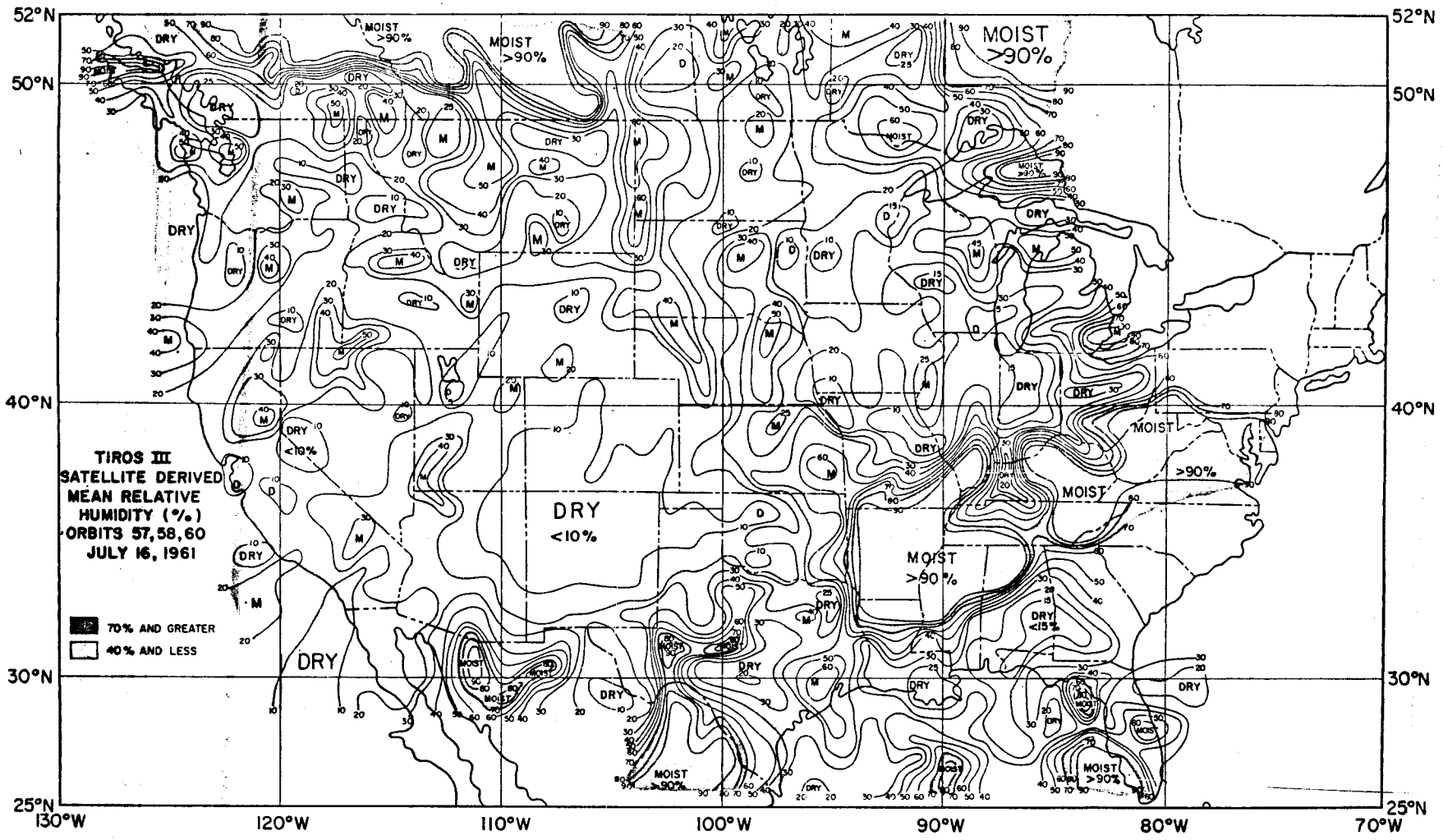
52°N
50°N
40°N
30°N
25°N
130°W
120°W
110°W
100°W
90°W
80°W
70°W
TIROS III
SATELLITE DERIVED
MEAN RELATIVE
HUMIDITY (%)
ORBITS 57, 58, 60
JULY 16, 1961
70% AND GREATER
40% AND LESS
MOIST >90%
DRY <10%
DRY

Fig. 10

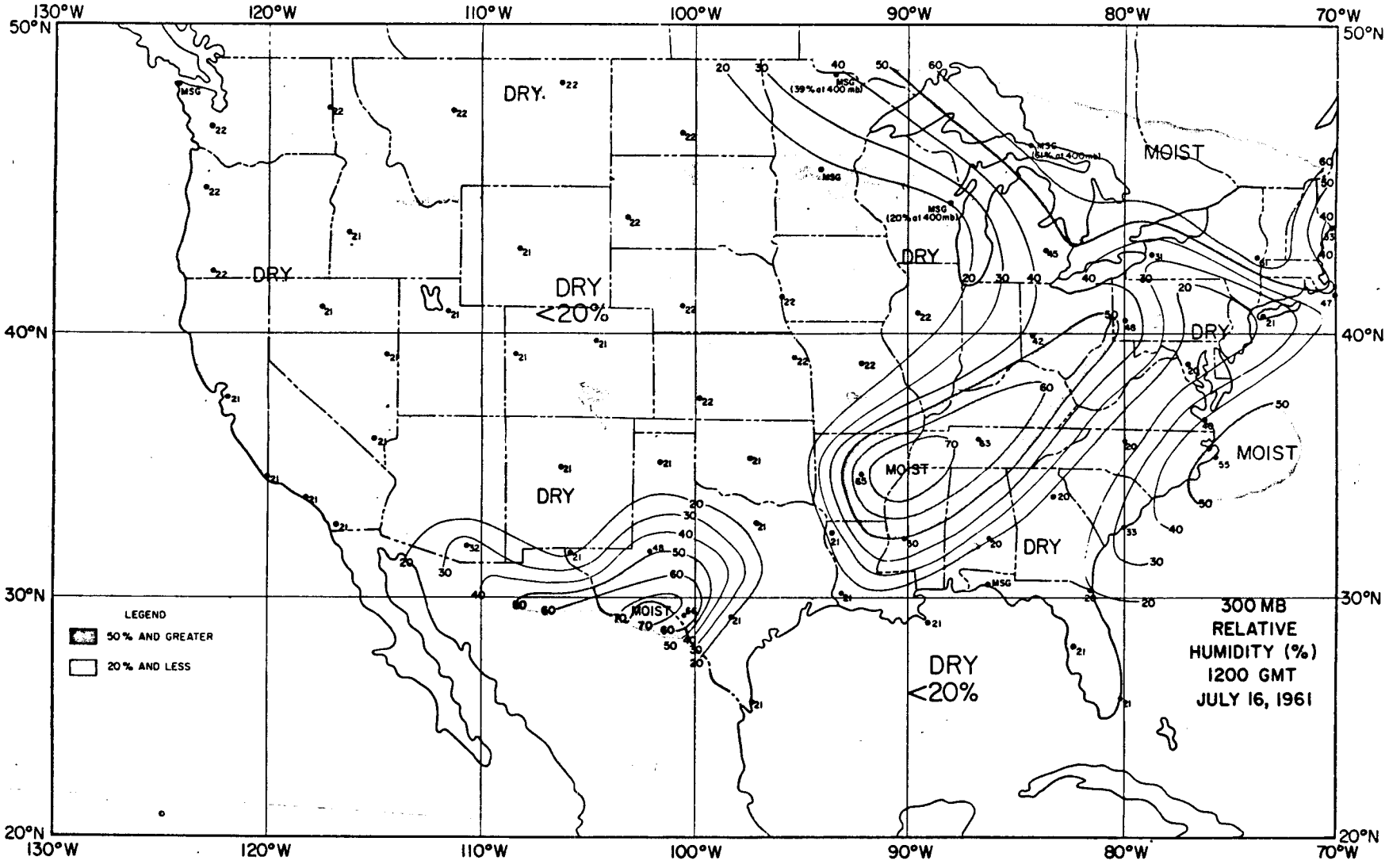
130°W
120°W
110°W
100°W
90°W
80°W
70°W
50°N
40°N
30°N
20°N
DRY
DRY
<20%
DRY
MOIST
DRY
MOIST
MOIST
DRY
DRY
<20%
MOIST
LEGEND
50% AND GREATER
20% AND LESS
300 MB
RELATIVE
HUMIDITY (%)
1200 GMT
JULY 16, 1961

Fig 11

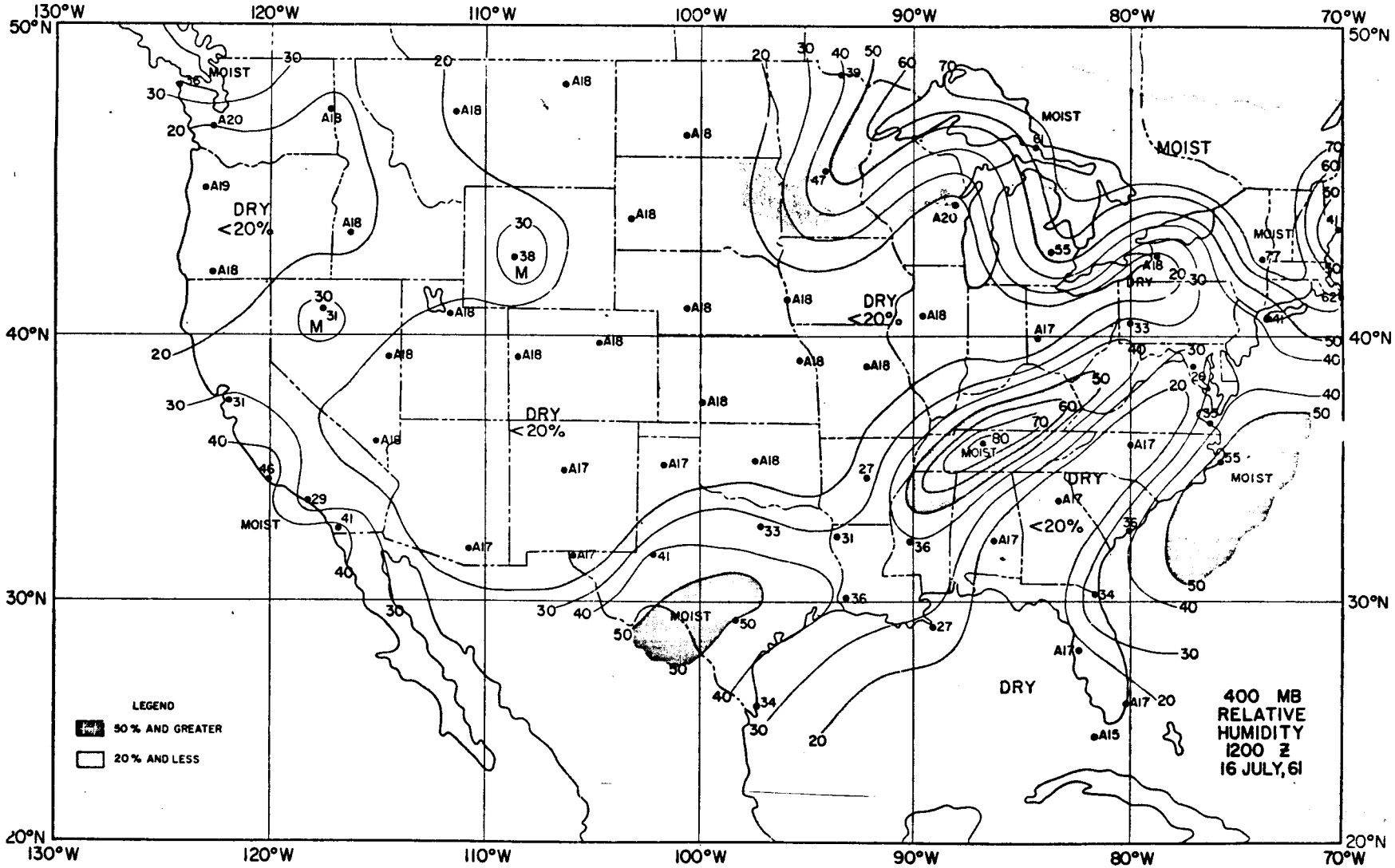
130°W
120°W
110°W
100°W
90°W
80°W
70°W
50°N
40°N
30°N
20°N
DRY
<20%
MOIST
LEGEND
50% AND GREATER
20% AND LESS
400 MB
RELATIVE
HUMIDITY
1200 Z
16 JULY, 61

Fig 12

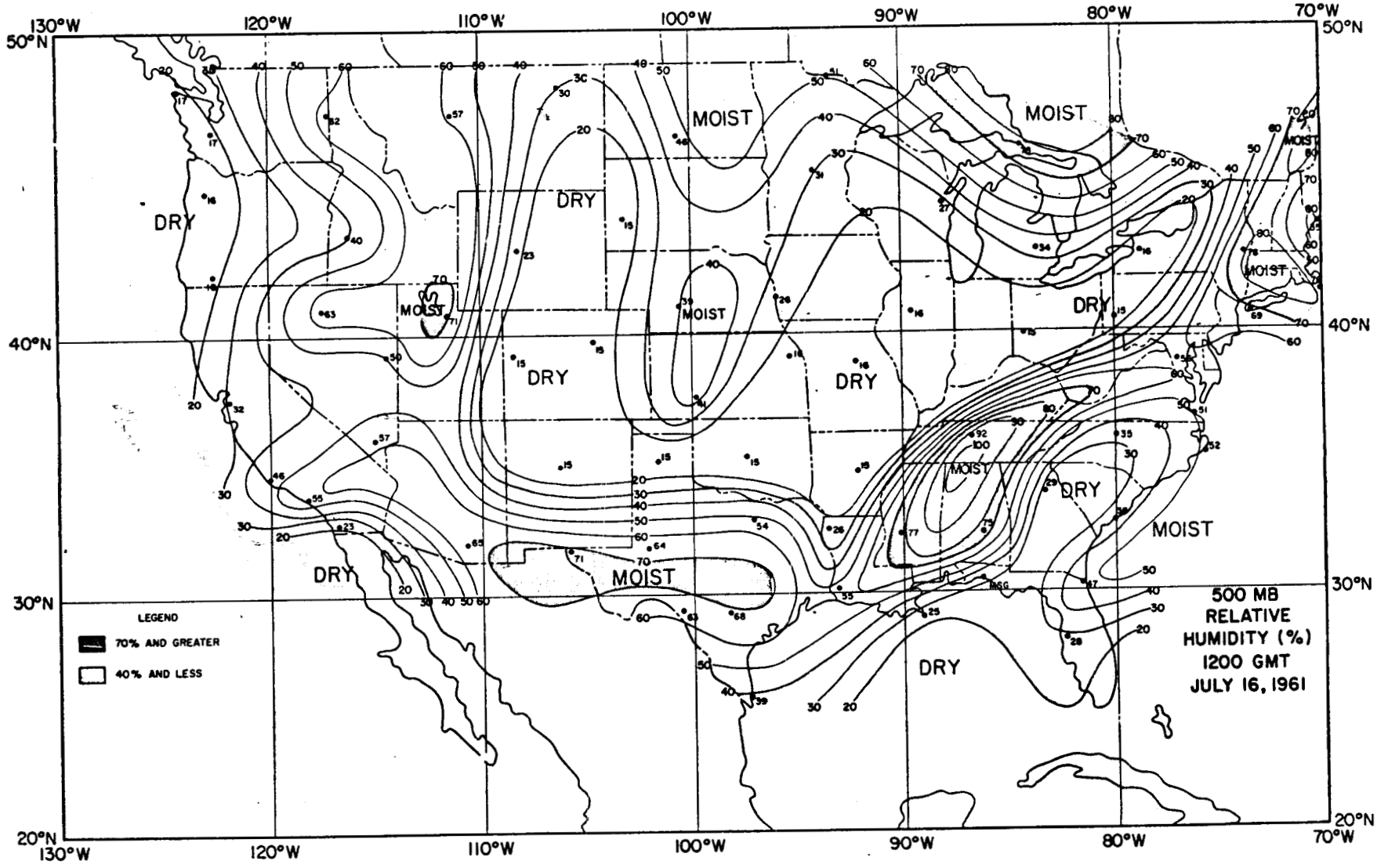
130°W
120°W
110°W
100°W
90°W
80°W
70°W
50°N
40°N
30°N
20°N
DRY
MOIST
LEGEND
70% AND GREATER
40% AND LESS
500 MB
RELATIVE
HUMIDITY (%)
1200 GMT
JULY 16, 1961

Fig. 13

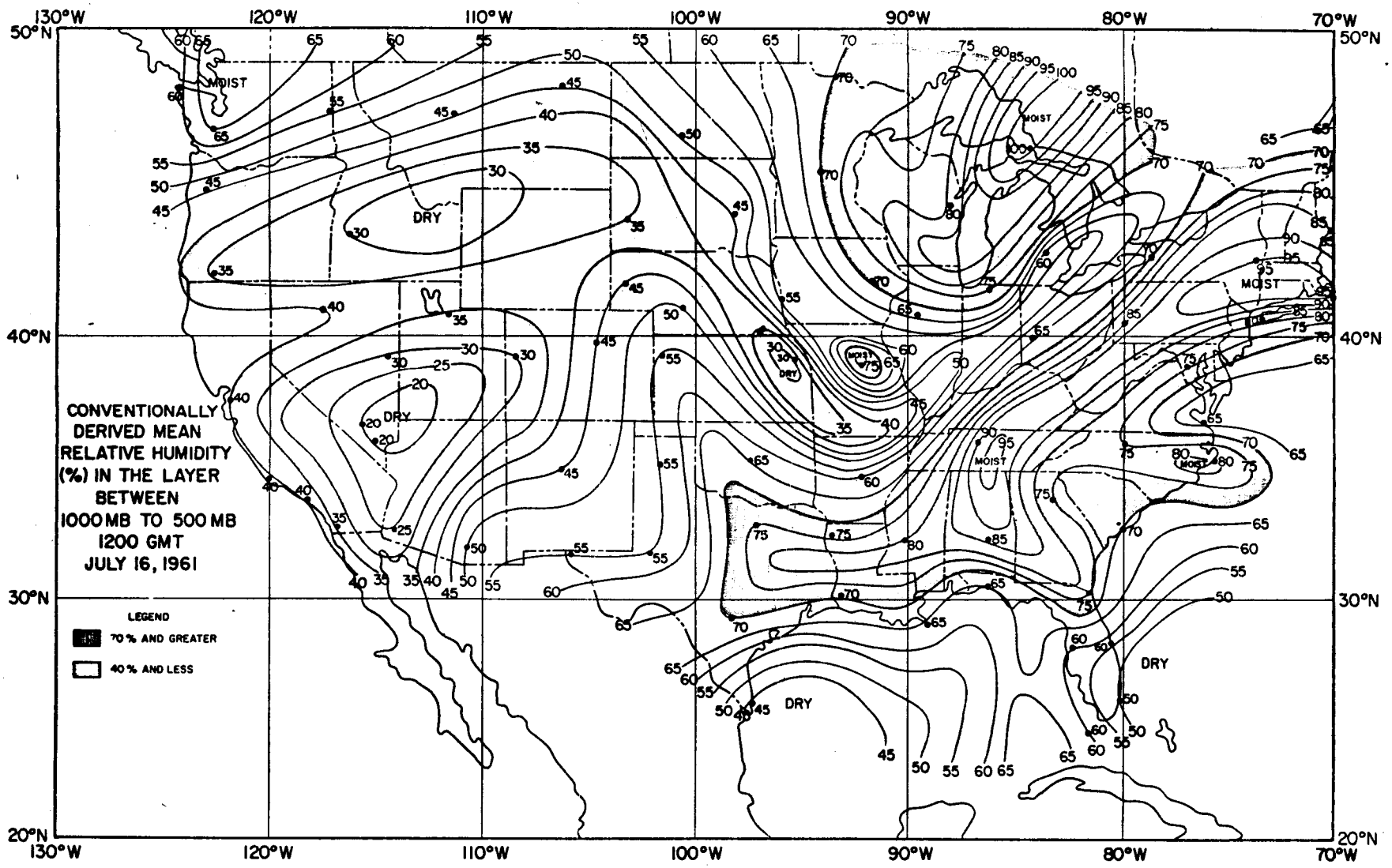
130°W
120°W
110°W
100°W
90°W
80°W
70°W
50°N
40°N
30°N
20°N
CONVENTIONALLY DERIVED MEAN RELATIVE HUMIDITY (%) IN THE LAYER BETWEEN 1000 MB TO 500 MB 1200 GMT JULY 16, 1961
LEGEND
70 % AND GREATER
40 % AND LESS
MOIST
DRY

Fig. 14

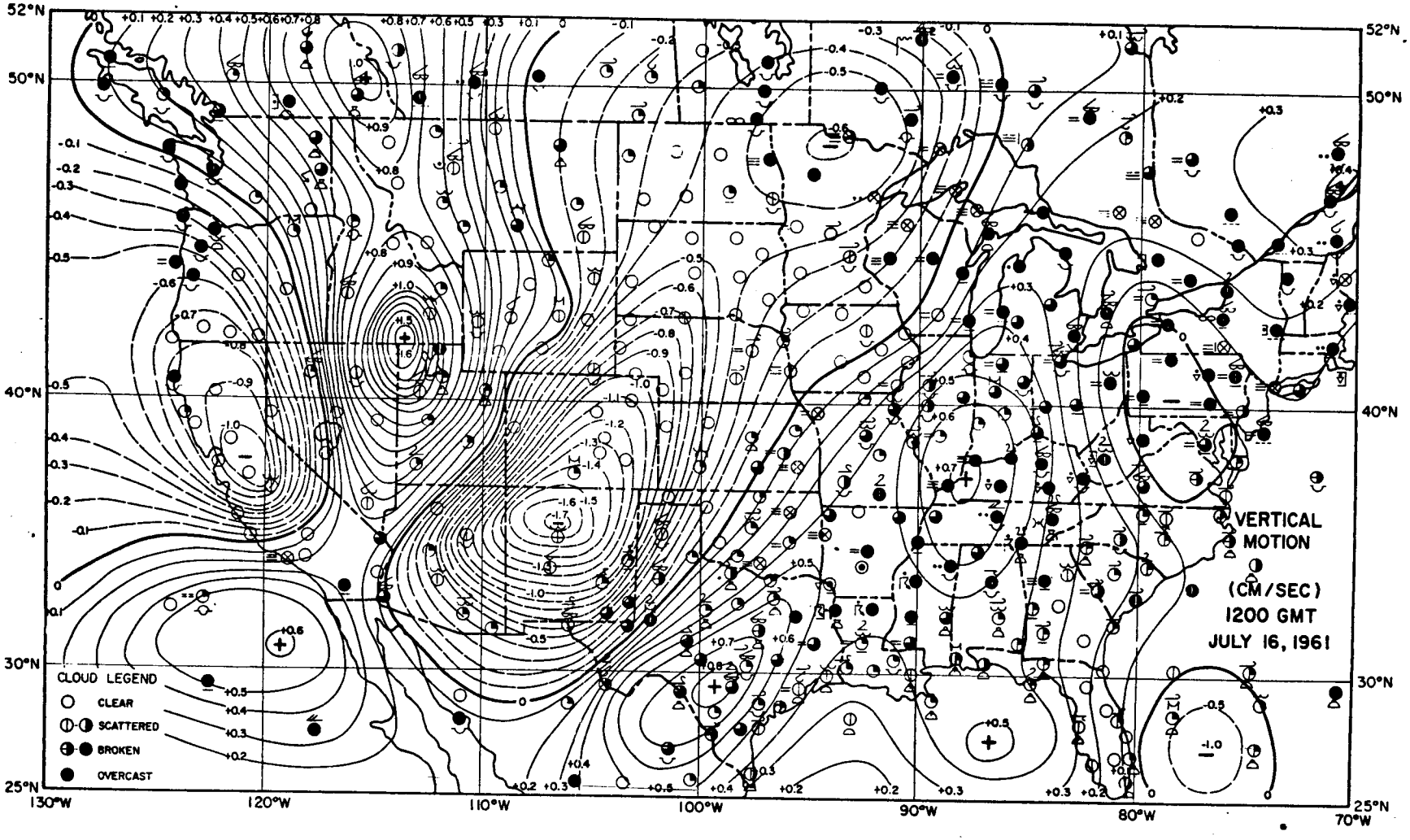
52°N
50°N
40°N
30°N
25°N
130°W
120°W
110°W
100°W
90°W
80°W
70°W
VERTICAL MOTION
(CM/SEC)
1200 GMT
JULY 16, 1961
CLOUD LEGEND
CLEAR
SCATTERED
BROKEN
OVERCAST

Fig. 15

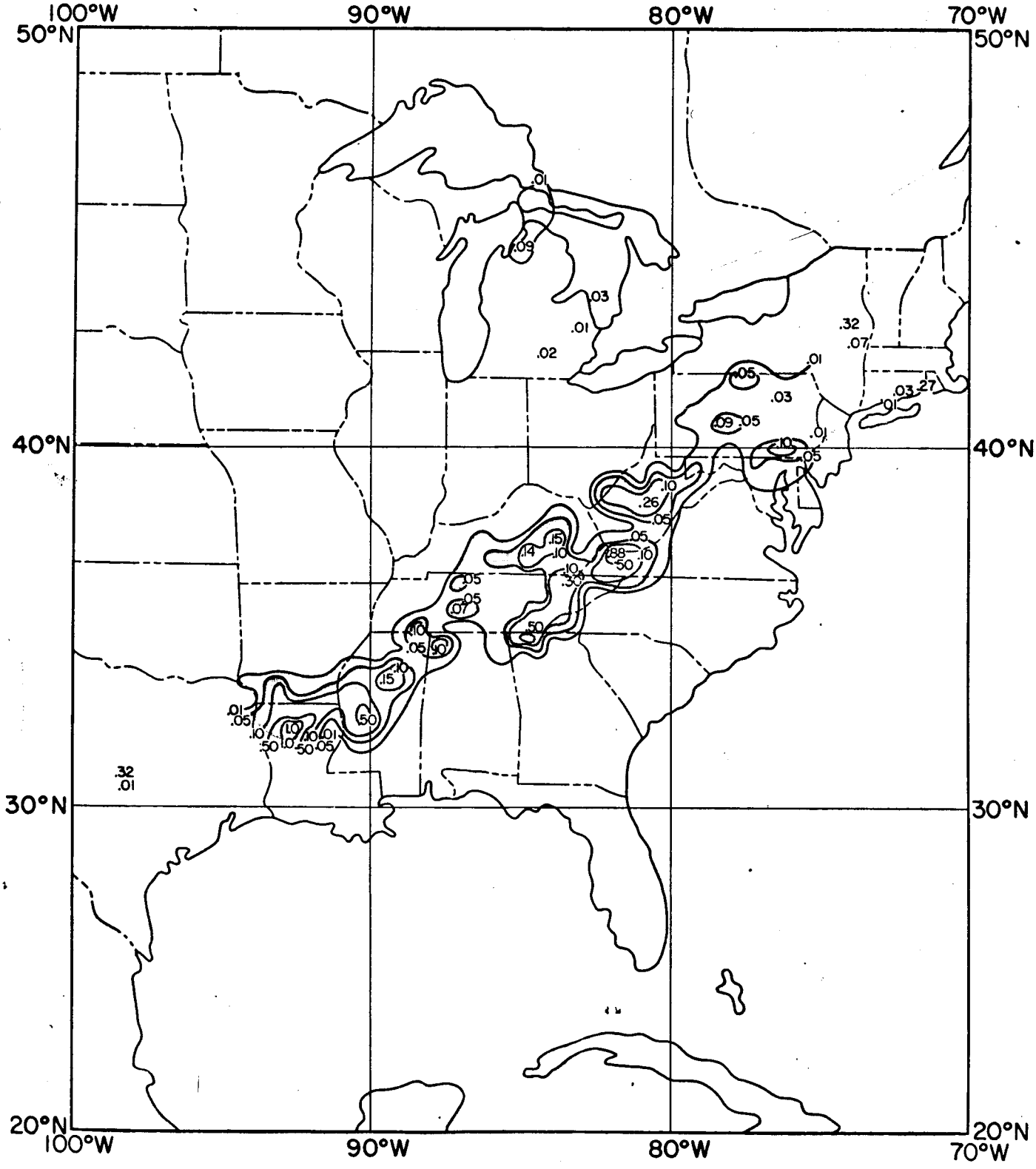

Fig. 16

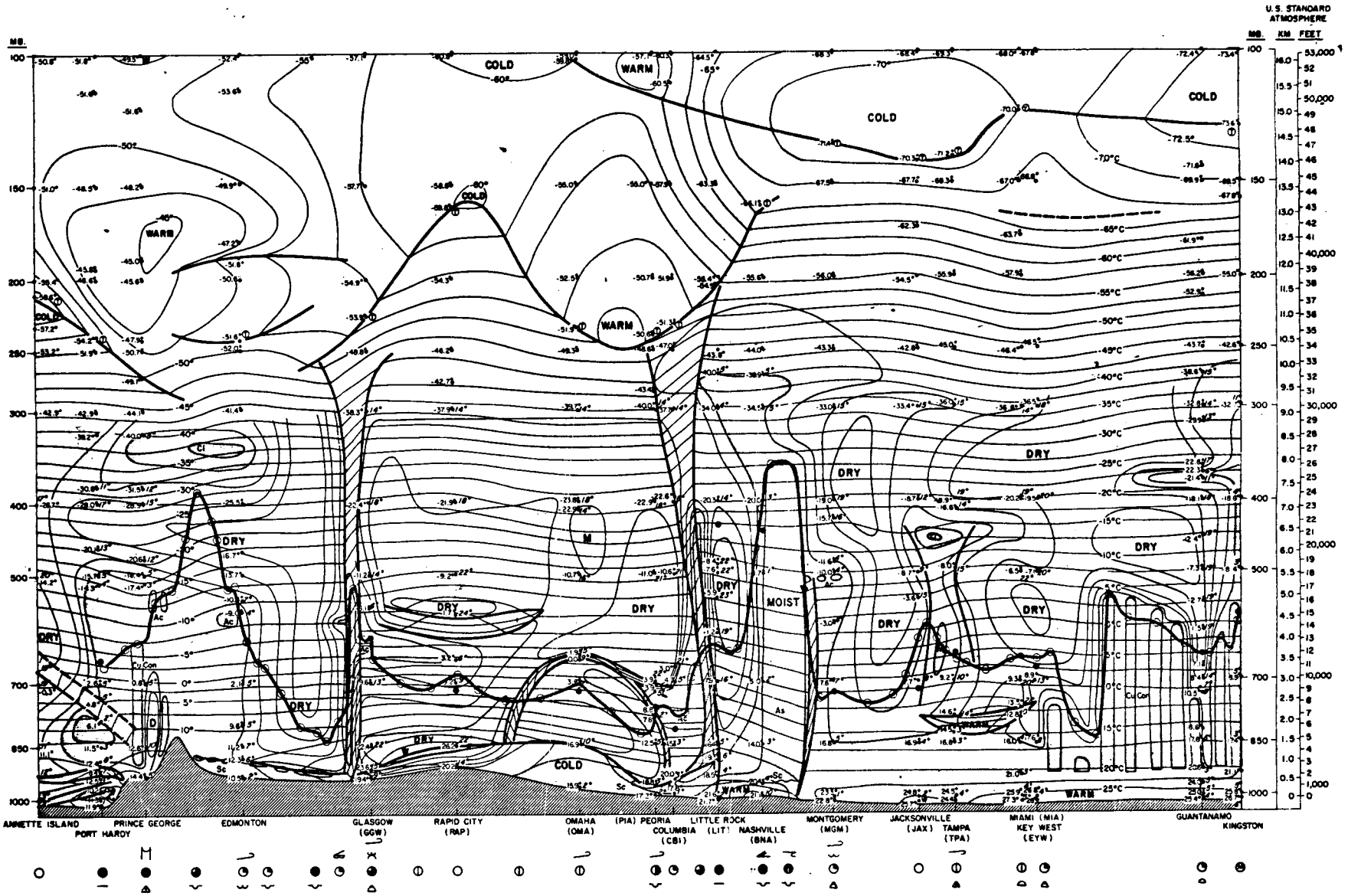
U.S. STANDARD ATMOSPHERE
MB.
MB.
KM
FEET
COLD
WARM
DRY
MOIST
ANNETTE ISLAND
PORT HARDY
PRINCE GEORGE
EDMONTON
GLASGOW (GGW)
RAPID CITY (RAP)
OMAHA (OMA)
(PIA) PEORIA
COLUMBIA (CBI)
LITTLE ROCK (LIT)
NASHVILLE (BNA)
MONTGOMERY (MGM)
JACKSONVILLE (JAX)
TAMPA (TPA)
MIAMI (MIA)
KEY WEST (EYW)
GUANTANAMO
KINGSTON

Fig. 17

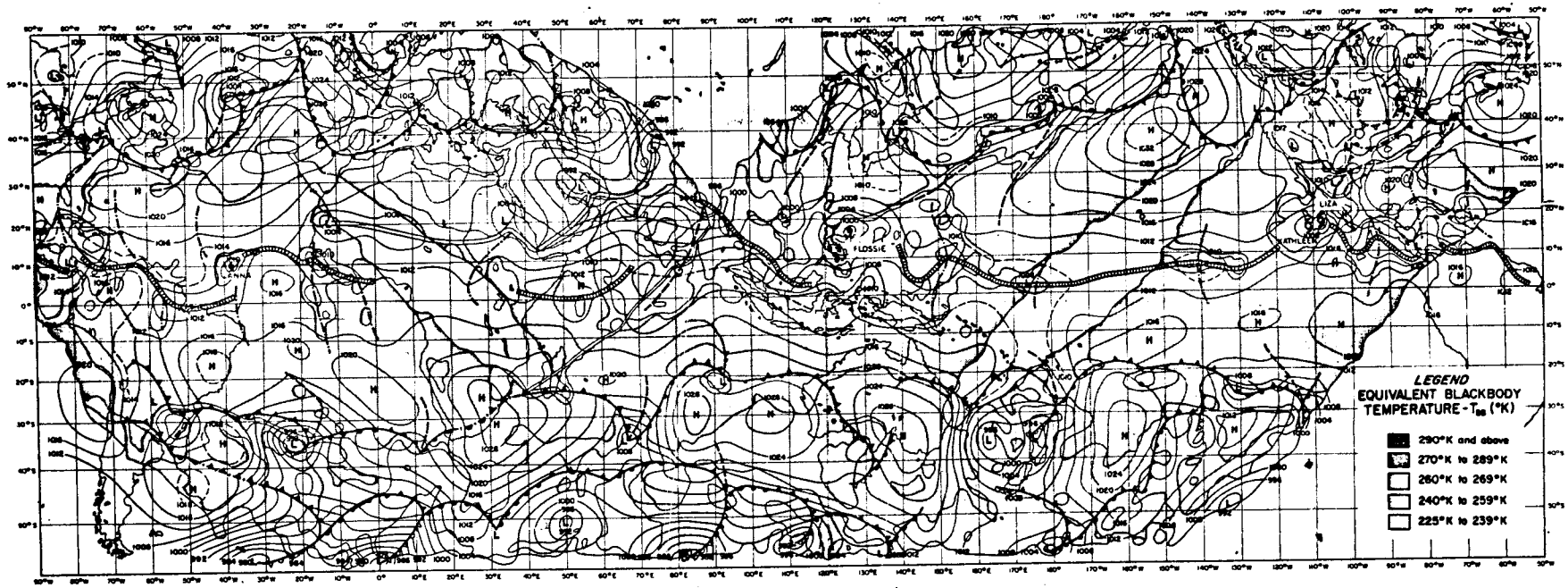
LEGEND
EQUIVALENT BLACKBODY
TEMPERATURE - T_{BB} (°K)
290°K and above
270°K to 289°K
260°K to 269°K
240°K to 259°K
225°K to 239°K
FLOSSIE
LIZA
KATHLEEN

Fig. 18